

Identification of Topography of Surfaces Created by Turning Biomaterials with Optical Profilometry

Zuzana Mital'ová,^{a,*} Dušan Mital',^a František Botko,^a Juliána Litecká,^b Jozef Zajac,^a Marta Harničárová,^{c,d} and Jan Valíček^{c,d}

This study deals with the identification of the topography of the surface that is created by machining composite materials with natural fibres (biomaterials, wood-plastic composites – a material with plastic matrix and natural reinforcement). The final surface was evaluated based on tool geometry (turning technology), and the influence of the tool on selected evaluating parameters of the obtained surface was evaluated using a non-contact method, applying an optical profilometer (MicroProf FRT). After machining the surface, characteristic relief (a trace on the surface of the material) was visible depending on the machining factors combination (machine, tool, workpiece, and fixture). The initial material also played a prominent role in the surface monitoring, in relationship to the composition of the material and the interaction between the matrix and reinforcement, *i.e.*, detection of defects in the area of the interaction between the initial components.

Keywords: Natural reinforcement; Wood-plastic composite; Topography of surface

Contact information: a: Department of Automotive and Manufacturing Technologies, Faculty of Manufacturing Technologies of Technical University of Kosice with seat in Presov, Sturova 31, 08001 Presov, Slovakia; b: Faculty of Humanities and Natural Science, University of Presov in Presov, Ul. 17. Novembra 1, 08001 Presov, Slovakia; c: Department of Mechanical Engineering, Institute of Technology and Business in Ceske Budejovice, Okruzni 10, 370 01 Ceske Budejovice, Czech Republic; d: Faculty of Engineering, Slovak University of Agriculture in Nitra, Tr. A. Hlinku 2, 949 76 Nitra, Slovakia;

* Corresponding author: zuzana.mitalova@tuke.sk

INTRODUCTION

Composite materials, such as wood-plastic composites (WPC), are formed by mixing two components of a polymer matrix and wood fibres (wood) in high content with the addition of additives. The price of wood flour is an insignificant factor compared to the price of thermoplastics. Therefore, an effort has been made to produce WPC materials with the highest possible content of organic components. It is possible to modify the mechanical properties of the final product *via* additives, such as lubricants, flame retardants, pesticides, pigments, and binders, by the amount and type of additive used, and without the use of toxins (Klyosov 2007; Niska and Sain 2008). The components are mixed at high temperature (below 400 °F, about $T_{\max} = 200$ °C) because wood fibres/particles decompose at a higher temperature, and application of the press extruder die enables their desired shape and size to be obtained. The final product properties depend on the components mentioned above and the manufacturing process itself. The WPC materials replace the traditional woods in the area of flooring, exterior cladding, or garden furniture because they provide: high durability, minimization of maintenance time, high dimensional stability, and resistance to weather and rot (Bailie 2004; Klyosov 2007; Niska and Sain 2008).

Although plastic is one of the main components of a WPC, external characteristics tend to be those of wood (appearance, texture, and feel when touched). For the production of a small number of pieces, the forming technology appears to be costly for the manufacture of a matrix of the required shape. Therefore, it is necessary to use conventional technologies: milling, turning, grinding, drilling, or cutting. When conventional technologies are used, the applied tool interacts with the material, creating a machined surface. There are numerous factors that affect the machined surface. Consequently, they also affect the set of characteristics referred to as technological inheritance, which are the properties and characteristics acquired after final technological processing. Through evaluating the set of these characteristics, the surface properties and the quality of the surface can be described, *i.e.*, with regards to topography. In general, the machinability of WPC materials is reported as “good” (Podziewski *et al.* 2018; Vinayagamorthy and Rajmohan 2018). However, the number of studies presented in this field is relatively low. The first studies in this field came from the Wood Machining and Tooling Research Program at North Carolina State University. In their work, the authors investigated the wear of carbide tools and the quality of the machined surface of WPC materials commercially used in the flooring industry compared to the machined wood sample after application of the grinding technology. Based on the results, they declared six times higher wear of carbide tools when machining WPC samples, compared to the machining of the sample made of pine. The assessed surface quality of the WPC and a wood pine sample was similar (Buehlmann *et al.* 2001).

Similarly, the authors (Guo *et al.* 2010) investigated the quality of the machined surface of WPC materials made from rice hull flour/polyethylene (PE), polypropylene (PP), and polyvinylchloride (PVC) after sawing, and Valarmathi and Palanikuma published a study on delamination in drilling of particleboard (wood composite panels) when changing the spindle speed, feed rate, and drill diameter. Their method of analysis was the Taguchi Technique (Valarmathi and Palanikuma 2013). This was followed by the works of Polish authors who created a machinability index for various types of WPC materials, compared to medium-density fibreboard (MDF) and standard particleboard, after drilling technology (Wilkowski *et al.* 2013), and studies dealing with the technology of turning, namely the influence of parameters of technological process on the quality of the machined surface – parameters stipulated the standard by STN EN ISO 4287 (1997) (Somsakova *et al.* 2012; Zajac *et al.* 2013; Mitalova *et al.* 2018). Recently, the possibility of machining these composite materials using the technology of abrasive water jet (AWJ)/water jet (WJ) (Hutyrova *et al.* 2016) has been opened. The results were presented in their work “Abrasive water jet turning of wood plastic composite”, in which they outlined the possibility of using WJ as an effective solution for roughing.

The objective of the present study was to supplement information on the topography of WPC plastic samples after turning as one of the indicators of technological inheritance. In the previous studies, only selected surface roughness parameters, R_a , R_z , *etc.*, were investigated (using the contact method). The studies were not focused on the texture or surface waviness (which is similarly significant in relation to the surfaces examined). By applying the non-contact optical profilometer method, it is possible to examine selected surfaces from multiple perspectives. The advantage is also the possibility to repeat measurements of selected parameters without the need of a contactless profilometer itself (images of samples are evaluated by software in a “home” PC).

EXPERIMENTAL

Materials and Methods

The investigated material (Germany) was plastic material filled with wood at a ratio of 25/75 (matrix – high-density polyethylene/wood filler) and particle size of 420 μm to 2 mm. The alignment of wooden particles followed the flow of mass during profile production. The material contained cracks located on the contact surface. Wood chips, as such, also contain isolated micro-cracks. A tensile test was performed according to ISO 6892 (2016) with a constant load speed of $0.015 \text{ mm}\cdot\text{s}^{-1}$. The tri-axial bend test was performed according to ISO 178 (2019) with a constant speed of $0.08 \text{ mm}\cdot\text{s}^{-1}$. Test samples, five pieces for each testing methodology, were taken along the extrusion axis from the central part of the profile. The tests were performed on a universal testing machine TIRA test 2300 (TIRA GmbH, Schalkau, Germany). The shape of the testing samples is shown in Figs. 1 and 2.

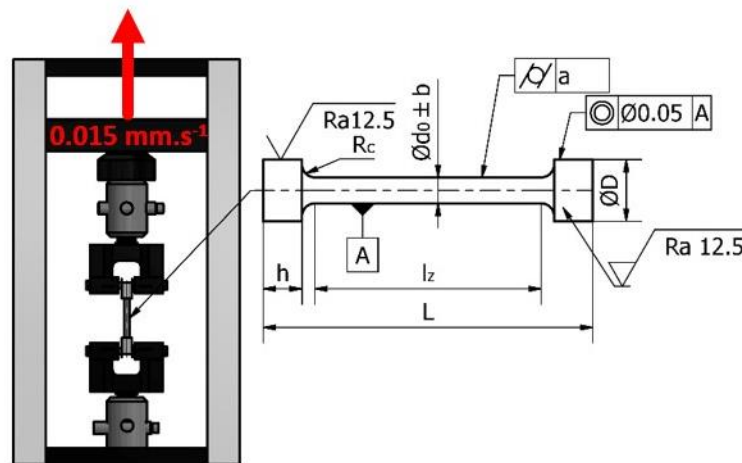


Fig. 1. The shape of the testing sample and testing method (tensile testing), the dimensions of a testing sample are specified in the standard ISO 6892 (2016)

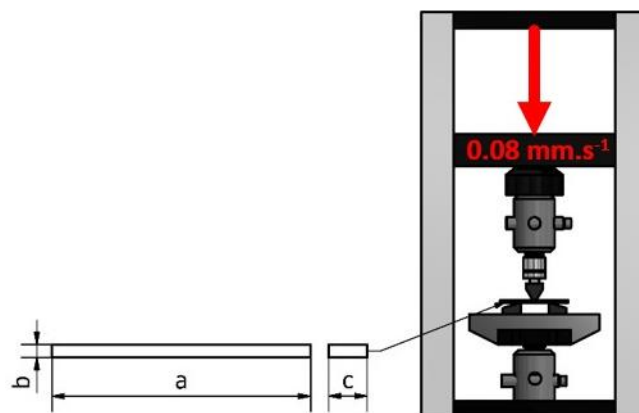


Fig. 2. The shape of the testing sample and testing method (bending test), the dimensions of a testing sample are specified in the standard ISO 178 (2019)

The values of mechanical properties are presented in Tables 1 and 2. Determination of deformation work was performed by integrating the load diagram. It was impossible to determine the yield strength correctly because conventional values of proof strain were not

available for the given type of material for the determination of inexpressive yield strength. Values of the mechanical properties of the five investigated samples varied greatly. The results clearly show that it is an inhomogeneous material (already on a macroscopic level).

Table 1. Values of Mechanical Properties after the Tensile Test

Tensile Strength (MPa)	Ductility (%)	Contraction (%)	Strain Energy (mJ)
19.0 (15 to 24)	3.55 (2.8 to 5.1)	0.9 (0.4 to 2.0)	17.6 (12.4 to 20.4)
Values are reported as an arithmetic mean of the four samples tested; sample No. 5 ruptured due to defect already at a load of 200 N; values given in parenthesis are the limits of the measured values			

Table 2. Values of Mechanical Properties after Tri-axial Bend Test

Bending Strength (MPa)	Strain Energy (mJ)
16.75 (15.44 to 18.76)	0.91 (0.8 to 1.01)
Values given in parenthesis are the limits of the measured values	

Conditions of the cutting process and sample identification

For experimental measurements, cutting tools made of high-speed steel – HSS (EN ISO HS6-5-2) with positive geometry and large tool nose radius $r_\epsilon = 5$ mm were used. During machining, two parameters were changed: feed per revolution f (mm) and spindle n (rpm). The cutting depth for final diameter was $a_p = 2.5$ mm (constant, from the original cross-section of 36 mm). Because the material was wood-based, machining was without cutting fluid. The samples were marked by feed per revolution and speed of rotation for tool X (a tool with an end relief angle $\alpha_p = 10^\circ$) and similarly marked samples were machined by tool Y (a tool with an end relief angle $\alpha_p = 15^\circ$) (Table 3).

Table 3. Conditions of the Cutting Process and Sample Identification

Sample Marking	Feed per revolution f (mm)	Speed of Rotation n (rpm)
X1 / Y1	0.1	450
X5 / Y5	0.61	450
X6 / Y6	0.1	900
X10 / Y10	0.61	900
X11 / Y11	0.1	1400
X15 / Y15	0.61	1400

Surface profile evaluation

For surface profile evaluation, an optical profilometer (MicroProf FRT; Fries Research & Technology GmbH, Bergisch Gladbach, Germany), based on chromatic aberration, was used to evaluate the surface topography (tool trace analysis). The turned samples were surface scanned and divided into two quadrants:

- Quadrant I: (Fig. 3) represented an area with formed anomalies, real measurements in this area might have led to misinterpretation of results;
- Surface scanning was performed in the area marked as quadrant II (without surface anomalies – Fig. 4).

The 3D images of surface topography were created from lines in the vertical and horizontal directions (400×400 lines). The distance between adjacent lines was 0.005 mm.



Fig. 3. Quadrant I –anomalies (cracks of the surface) formed



Fig. 4. Quadrant II – without any anomalies on the surface

Principle of operation of optical profilometer MicroProf FRT

The experimental evaluation of the surface profile was performed at the Faculty of Mechanical Engineering – Brno University of Technology (Brno, Czech Republic). The principle of operation of the profilometer MicroProf FRT with the optical sensor CHR 150N is shown in Fig. 5.

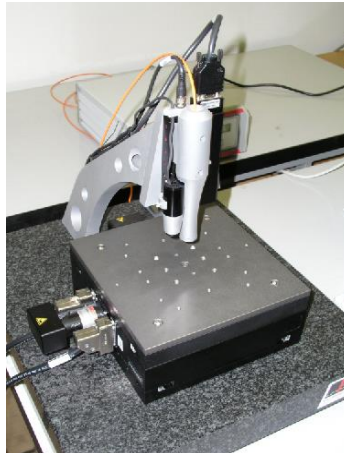


Fig. 5. General view of the optical profilometer MicroProf FRT

The white light from the source is led to the lens by an optical fibre. The lens, due to its sizeable chromatic aberration, focuses the individual monochromatic components of the white light to different heights above the reference plane. After impacting the investigated surface, the focused light is reflected into the lens, and subsequently, it is led by an optical fibre into the spectrometer. The wavelength value of the maximum light intensity output from the spectrometer is converted using a calibration table to the distance between the sensor and the investigated surface, by which information is obtained on the surface unevenness. The measurement process was performed by moving the sliding table on which the sample is placed (movement in x-y direction). The table advance is controlled by the processor in defined lines. It was evident from the described principle of operation that the sensor of the optical profilometer does not track by its movement on the surface

profile. However, it obtained the necessary data from each measurement point independently, which results in relatively high measurement accuracy. The measurement result takes the form of a vector of surface height unevenness values. The measurement software “Acquire” (Fries Research & Technology GmbH, Bergisch Gladbach, Germany) makes it possible to select the line or the measurement area, set the sensor to the desired position, and set the scanning parameters and file handling (Brillova *et al.* 2012; Zelenak 2012; Carach *et al.* 2016). The processing of the obtained data was performed with the use of the software Gwyddion (David Nečas and Petr Klapetek, v.2.36, Brno, Czech Republic). The basic parameters of MicroProf FRT were as follows: xy minimal range: $200 \times 200 \mu\text{m}^2$, xy maximum range: $(100 \times 100) \times 10^{-6} \mu\text{m}^2$, measurement range: $(300 \mu\text{m} - 3) \times 10^3 \mu\text{m}$, vertical resolution $3 \times 10^{-3} \mu\text{m}$, lateral resolution: $2 \mu\text{m}$, maximum angle of inclination of the surface roughness to the mean plane: 30° (Valicek *et al.* 2015, Zelenak 2012).

RESULTS AND DISCUSSION

The presented research was carried out using representative samples of given groups (assured repeatability of the measurement, the evaluated sample represents a given group of samples machined under the same conditions, with one tool). During the evaluation of the reliefs of samples X1 to Y15 (labelled based on tool geometry and cutting process conditions, Table 3), waviness profiles/logarithmic profiles of the surface waviness course were made (for better resolution and legibility, the y-axis is logarithmic.) The 3D images of the surface topography of the samples X1 and X6 are characterised by a distinctive trace caused by the passage of the turning tool over the workpiece (Fig. 6). In the 3D image of sample X11, the groove is not readable (compared to the two samples above). The waviness profile on the sample X1 exhibited differences of $5 \mu\text{m}$, which corresponded to approximately 20 times the theoretical camber calculated from two key parameters, rounding and the advance of the cutting edge Eq. 1 (in μm).

$$R_z = \frac{f^2}{8 \cdot r_\varepsilon} \cdot 1000 \quad (1)$$

where R_z is the maximum height of the profile (μm), f is the feed per revolution (mm), and r_ε is the tool nose radius (mm).

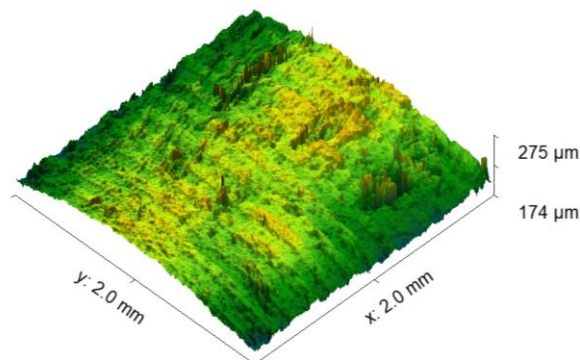


Fig. 6. 3D profile of sample X1 (significant tool trace, feed $f = 0.1 \text{ mm}$)

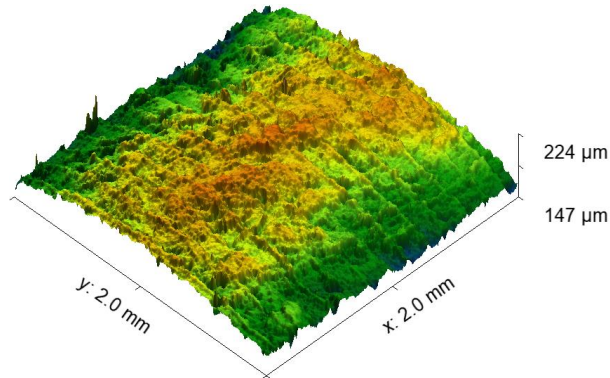


Fig. 7. 3D profile of sample X6 (significant tool trace, feed $f = 0.1$ mm)

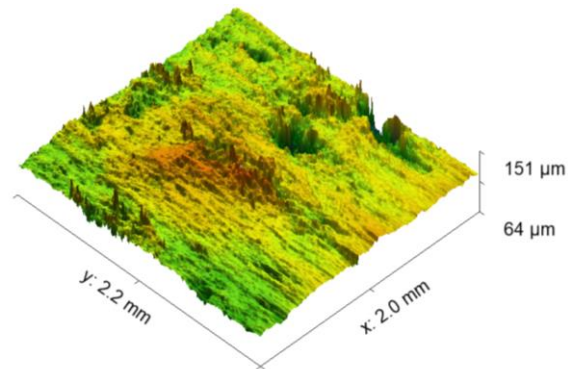


Fig. 8. 3D profile of sample X11 (tool trace insignificant, $f = 0.1$ mm)

The logarithmic evolution of waveform exhibited noticeable peaks, the number of which was identical to the number of passes of the tool in the observed area (2 mm in length, with an advance of 0.1 mm, the theoretical number of observed peaks is 20).

A similar logarithmic waveform is visible for samples labelled X6 and X11 - Figs. 10 and 11 - left (samples made with 0.1 mm feed).

For the group of samples Y1, Y6, and Y11 (Figs. 9 to 11 right), it was not possible to determine the number of transitions from the waveform on the basis of the previous consideration; because of the possibility of comparing samples machined under the same conditions, by two different tools, the logarithmic waveforms of the surface waviness are located in the pictures on the right and left.

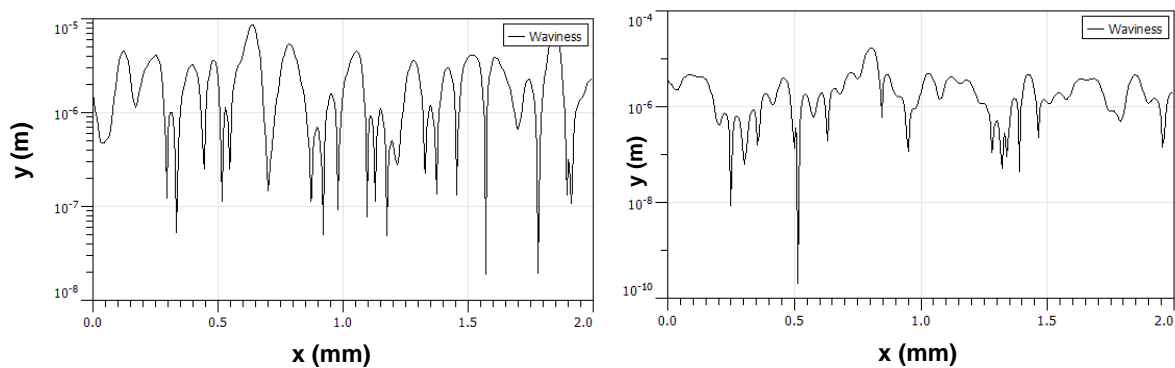


Fig. 9. Sample X1 surface waviness waveform – left; sample Y1 surface waviness waveform - right (logarithmic y-axis)

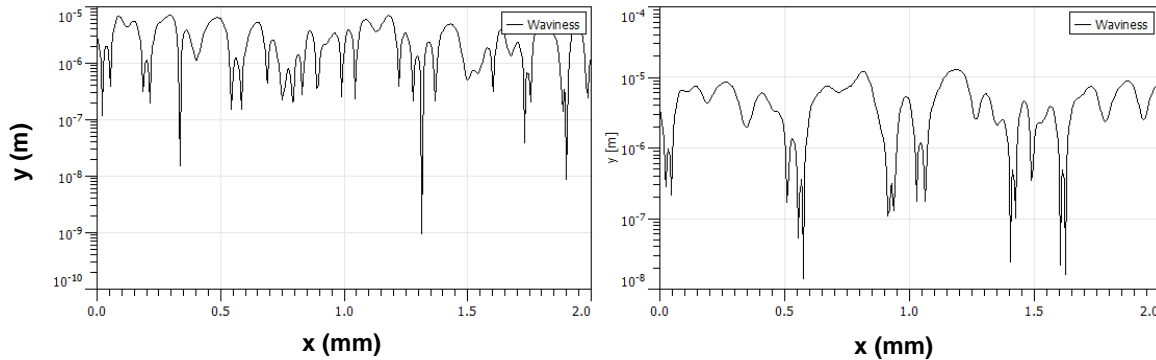


Fig. 10. Sample X6 surface waviness waveform – left; sample Y6 surface waviness waveform - right (logarithmic y-axis)

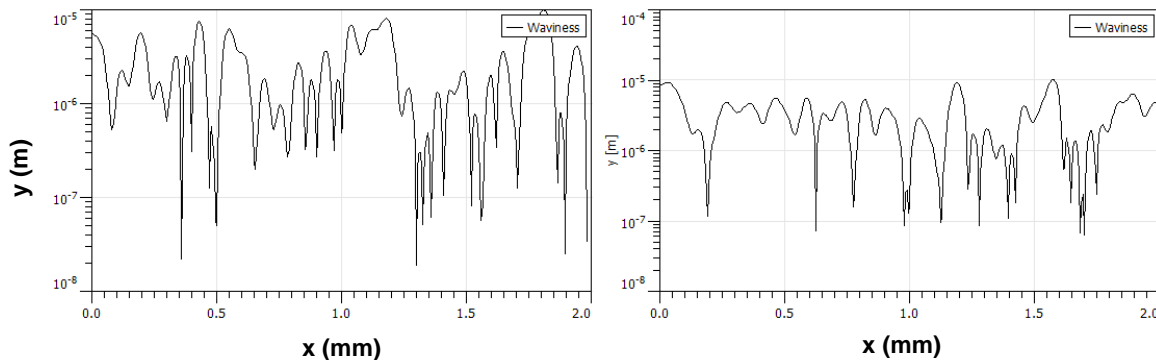


Fig. 11. Sample X11 surface waviness waveform – left; sample Y11 surface waviness waveform - right (logarithmic y-axis)

With respect to the geometry of the tool, it can be said that: samples of group Y - located to the right in Figs. 9 to 11 (Y1, Y6, Y11 - machined with a tool with an end relief angle of 15°) showed a higher surface quality, as there were less noticeable traces of individual tool passes). This was due to a bigger end relief angle and thus smaller interaction of the newly formed surface with the tool.

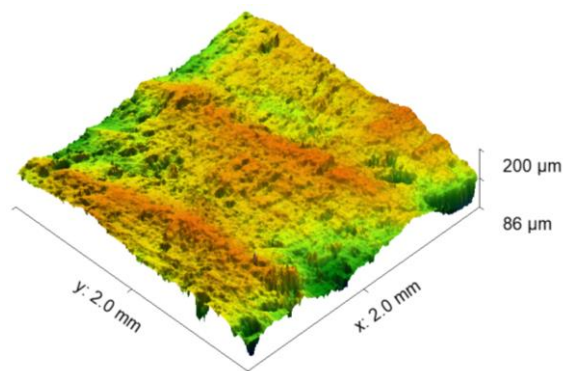


Fig. 12. 3D profile of sample X5 (feed $f = 0.61$ mm)

The 3D surface profile of sample X5 is shown in Fig. 12. Samples made at a maximum feed of 0.61 mm can be seen in Figs. 13 to 15. Samples Y5 and Y15 (Figs. 13 and 15 right) confirm that samples machined with a tool with a 15° end relief angle exhibited a higher surface quality compared to samples machined with a tool with a 10° end relief angle (compared to samples X5 and X15). This was not true for samples X10

and Y10 (Fig. 14). The resulting surface topography was influenced in addition to the aforementioned parameters of the tool and its advance also by other factors, *i.e.*, machine, tool, or workpiece. The most noticeable impact on the surface of these factors was the material of the workpiece. Due to the inhomogeneity of the material (already at the macroscopic level), the quality of the machined surface was largely dependent on the distribution of the wood fibres in the plastic binder. Therefore, it was difficult to compare the quality of the machined surface with the quality of the surface achieved when machining homogeneous materials. During WPC machining, build-ups are formed (on a turning tool) of the binder material, and at the same time, wood fibres are pulled out of the machined surface.

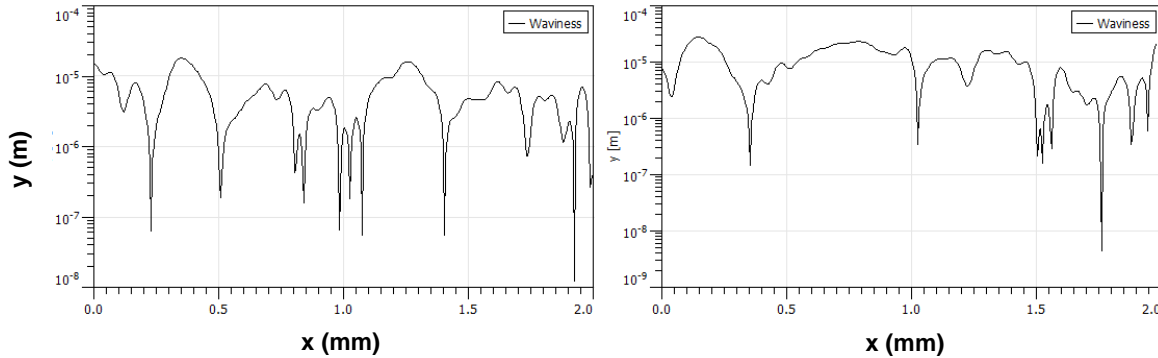


Fig. 13. Sample X5 surface waviness waveform – left, sample Y5 surface waviness waveform - right (logarithmic y-axis)

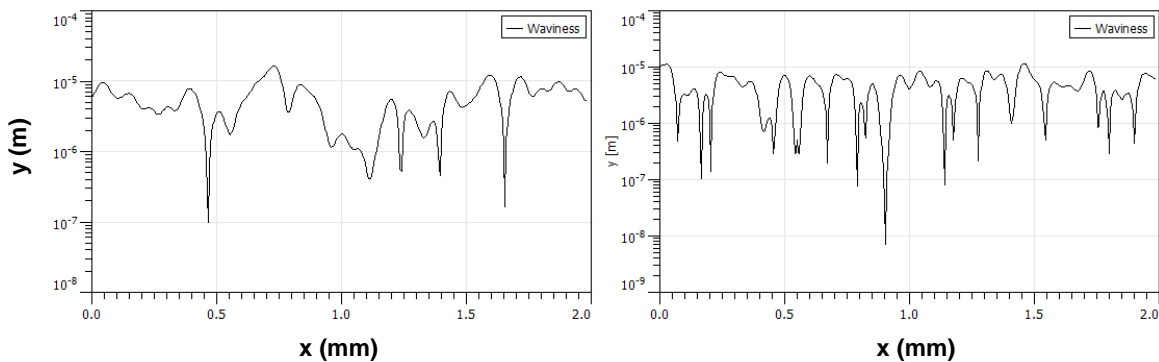


Fig. 14. Sample X10 surface waviness waveform – left, sample Y10 surface waviness waveform - right (logarithmic y-axis)

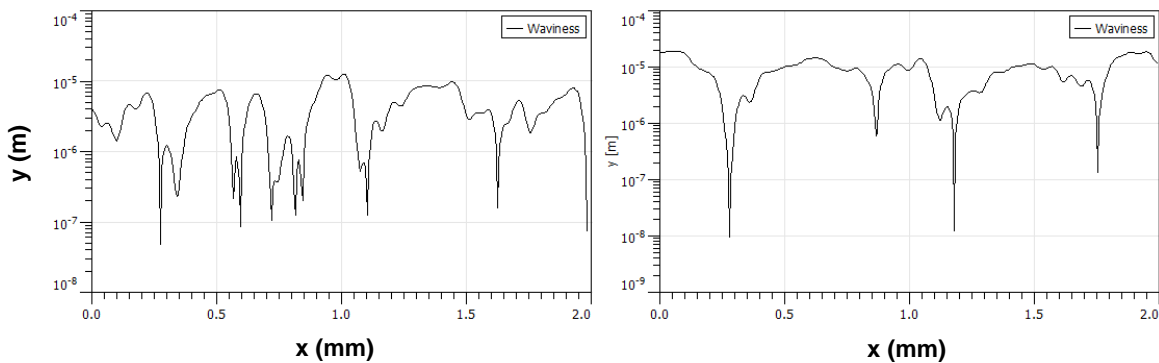


Fig. 15. Sample X15 surface waviness waveform – left, sample Y15 surface waviness waveform - right (logarithmic y-axis)

CONCLUSIONS

This study investigated the identification of topography of the surface created by turning biomaterials (natural-based composite materials).

1. In the process of evaluation of the surface topography, two factors play a prominent role for WPC materials: feed per revolution – f (as one of the conditions of the cutting process) and the tool nose radius – r_e . In the logarithmic evolution of waveform, the advance is shown by distinct peaks. However, the issue of evaluation of the surface topography after machining needs to be understood comprehensively.
2. The surface after cutting also depends on the interaction of factors of the technological system (machine – tool – workpiece – fixture). Of these functional factors, the workpiece material (which is characterised as inhomogeneous) is of noticeable importance.
3. The surfaces created with a tool with a 10° end relief angle exhibit a clear trace of tool pass, and in the logarithmic evolution of waveform, it was also possible to observe peaks that copy the number of tool passes. The plastic component of the WPC material is cushioned, causing an additional contact of the tool with the machined surface behind the cutting edge.
4. The surfaces created by a tool with a 15° end relief angle show a less noticeable trace of the individual tool passes, and the logarithmic evolutions of waveforms of the surface do not copy markedly individual passes of the tool. When using a tool with a 15° end relief angle, it can be stated that there is no noticeable interaction of the tool with the newly formed surface behind the cutting edge. Thus, the surface was more affected by the inhomogeneity of the machined material and by the random distribution of the wood filler in the plastic material matrix.
5. The main idea of the presented research was to evaluate the topography of the surface created by a single-wedge tool when machining rotary surfaces of a composite material with natural reinforcement. Machining wood-composite materials is specific in view of the significant heterogeneity of the material formed by the polymer matrix and the wood flour filler. Due to this inhomogeneity, there are several mechanisms in machining that do not occur when machining metals. A prevalent mechanism that accompanies the machining of WPC is pulling the wood particles out of the matrix. The second distinct mechanism is the melting of the polymer matrix. These phenomena result in a different surface topography than expected based on the theory of machining according to the relationship (1). Based on the research carried out, it seems preferable to use a larger end relief angle. Because the polymer matrix is prone to cushioning, a larger end relief angle allows the tool to contact the workpiece beyond the cutting edge to achieve better results in terms of surface topography of the machined surface.

ACKNOWLEDGEMENTS

This work was supported by the project KEGA 030TUKÉ-4/2018 (Popularization of Industry 4.0 and Digitization Enterprises Problematic as a Tool for Increase of Technical

Knowledge and Skills by Students of Secondary School). This work was supported by the Slovak Research and Development Agency under the contract No. APVV-15-0700.

REFERENCES CITED

- Bailie, C. (2004). "Life cycle assessment," in: *Green Composites, Polymer Composites and the Environment*, CRC Press, Boca Raton, FL, USA, pp. 23-47.
- Brililova, K., Ohlidal, M., Valiček, J., Kozak, D., Zelenák, M., Harničárová, M., and Hlaváček, P. (2012). "Spectral analysis of metallic surfaces topography generated by abrasive waterjet," *Tehnicki Vjesnik* 19(1), 1-9.
- Buehlmann, U., Saloni, D., and Lemaster, R. L. (2001). *Wood Fiber-Plastic Composites: Machining and Surface Quality*, in: *15th International Wood Machining Seminar*, Anaheim, CA, USA, pp. 1-13.
- Carach, J., Hloch, S., Hlaváček, P., Gombár, M., Klichová, D., Botko, F., Mitaľ, D., and Lehocká, D. (2016). "Hydro-abrasive disintegration of alloy Monel K-500-the influence of technological and abrasive factors on the surface quality," in: *International Conference on Manufacturing Engineering and Materials*, Nový Smokovec, Slovakia, pp. 17-23.
- Hutyrova, Z., Ščučka, J., Hloch, S., Hlaváček, P., and Zelenák, M. (2016). "Turning of wood plastic composites by water jet and abrasive water jet," *International Journal of Advanced Manufacturing Technology* 84(5-8), 1615-1623. DOI: 10.1007/s00170-015-7831-6
- ISO 178 (2019). "Plastics -- Determination of flexural properties," International Organization for Standardization, Geneva, Switzerland.
- ISO 6892 (2016). "Metallic materials -- Tensile testing -- Part 1: Method of test at room temperature," International Organization for Standardization, Geneva, Switzerland.
- Klyosov, A. A. (2007). "Foreword- Overview: Wood-plastic composites," in: *Wood-Plastic Composites*, John Wiley & Sons, Hoboken, NJ, USA, pp. 11-48.
- Mitaľová, Z., Mitaľ, D., Botko, F., Litecká, J., Harničárová, M., Valiček, J., and Ohlidal, M. (2018). "Influence of factors on surface topography of wood-based composite material," *Academic Journal of Manufacturing Engineering* 16(4), 110-114.
- Niska, K. O., and Sain, M. (2008). "Outdoor durability of wood-polymer composites," in: *Wood-polymer Composites*, Woodhead Publishing Limited, Cambridge, England, pp. 142-162.
- Ohlidal, M. (2018). "Opticke metody hodnoceni textury povrchu v mikrometrove oblasti [Optical methods of surface texture evaluation in micrometer area]," (https://ecitydoc.com/download/opticke-metody-hodnoceni-textury-povrchu-v_pdf), Accessed 28 July 2018.
- Podziewski, P., Szymanowski, K., Górki, J. and Czarniak, P. "Relative machinability of wood-based boards in the case of drilling – Experimental study," *BioResources* 13(1), 1761-1772.
- Somsakova, Z., Zajac, J., Michalik, P., and Kasina, M. (2012). "Machining of wood plastic composite (pilot experiment)." *Materiale Plastice* 49(1), 55-57.
- STN EN 4287 (1997). "Geometrical product specifications (GPS). Surface texture: Profile method - Terms, definitions and surface texture parameters," International Organization for Standardization, Geneva, Switzerland.

- Valarmathi, T. N., and Palanikumar, K. (2013). "Studies on delamination in drilling of particleboard (PB) wood composite panels," in: *Proceedings of the Indian National Science Academy* 79(3), 339-345.
- Valíček, J., Harničárová, M., Öchsner, A., Hutyrová, Z., Kušnerová, M., Tozan, H., Michenka, V., Špelák, V., Mitaľ, D., and Zajac, J. (2015). "Quantifying the mechanical properties of materials and the process of elastic-plastic deformation under external stress on material," *Materials* 8(11), 7401-7422. DOI: 10.3390/ma8115385
- Vinayagamorthy, R., and Rajmohan, T. (2018). "Machining and its challenges on bio-fibre reinforced plastics: A critical review," *Journal of Reinforced Plastics and Composites* 37(16), 1037-1050. DOI: 10.1177/0731684418778356
- Zajac, J., Hutyrová, Z., and Tarasovičová, A. (2013). "Assessment of statistical signification of factors by machining inhomogeneous materials - WPC," *Applied Mechanics and Materials* 308, 165-169. DOI: 10.4028/www.scientific.net/AMM.308.165
- Zelenak, M. (2012). *Measurement and Analysis of Topography of Cutting Walls Created by Abrasive Water Jet and CO₂ Laser in Terms of Material and Mechanism Disintegration*, PhD Dissertation, Faculty of Mining and Geology of Technical University of Ostrava, Ostrava, Czech Republic.
- Wilkowski, J., Borysiuk, P., Górski, J., and Czarniak, P. (2013). "Analysis of relative machinability indexes of wood particle boards bonded with waste thermoplastics," *Drewno* 56(190), 139-144. DOI: 10.12841/wood.1644-3985.039.09

Article submitted: October 14, 2019; Peer review completed: January 23, 2020; Revised version received and accepted: February 12, 2020; Published: February 17, 2020.
DOI: 10.15376/biores.15.2.2483-2494